JOURNAL OF ENVIRONMENTAL SCIENCES 138 (2024) 266–276

Available online at www.sciencedirect.com

ScienceDirect

www.elsevier.com/locate/jes

JES JOURNAL OF ENVIRONMENTAL SCIENCES

www.jesc.ac.cn

Assessment of tree-ring mercury radial translocation and age effect in Masson pine: Implications for historical atmospheric mercury reconstruction

Xu Liu[1], *Xun Wang*[2], *Dingyong Wang*[1,*]

[1] *College of Resources and Environment, Southwest University, Chongqing 400715, China*
[2] *State Key Laboratory of Environmental Geochemistry, Institute of Geochemistry, Chinese Academy of Sciences, Guiyang 550081, China*

ARTICLE INFO

Article history:
Received 21 September 2022
Revised 13 October 2022
Accepted 16 October 2022
Available online 27 October 2022

Keywords:
Masson pine
Tree-ring mercury
Radial translocation
Tree age effect

ABSTRACT

The tree ring has been regarded as an emerging archive to reconstruct historical atmospheric mercury (Hg) trends, but with the large knowledge gaps in the reliability. In this study, we comprehensively evaluated the Hg source, radial translocation and age effect of Masson pine (*Pinus massoniana*) tree ring at Mt. Jinyun in Chongqing, to assess the suitability of such tree ring as the archive of atmospheric Hg. Results showed that distinct variabilities among Masson pine tree-ring Hg concentration profiles. The Hg concentration significantly increased along with stem height ($P < 0.05$), indicating the Hg in tree rings mainly derived from foliage uptake atmospheric Hg. We found a distinct age effect that the tree ring of young trees had the higher Hg concentration. Besides, we used the advection-diffusion model to demonstrate how Hg concentration shifted by the advection or/and diffusion in tree rings. The modeling results showed that the advection induced radial translocation during the young growth period of tree was a plausible mechanism to result in the tree-ring Hg record largely different from the trend of anthropogenic Hg emissions in Chongqing. We finally suggest that in further Hg dendrochemistry, better discarding the tree-ring Hg profile of the young growth period to reduce impacts of the radial translocation and age effect.

Introduction

Mercury (Hg) is a global pollutant that is released into the atmosphere through various natural and anthropogenic sources. A cumulative total of anthropogenic 470 Gg of Hg has been emitted directly into the atmosphere since 1850s, 74% of which as the form of elemental Hg (Streets et al., 2017). Gaseous elemental mercury (GEM) has a 0.3- to 1.5- year atmospheric residence time which allows for the long-range transport of Hg^0 to deposit into remote regions (Lehnherr, 2014; Shah et al., 2021). The deposited Hg can be converted into the more toxic form, i.e., methyl-Hg in the certain environment, leading to the degradation of the environmental quality and human health (Chen et al., 2018; Lehnherr, 2014). To protect environment and human health from the global Hg pollution, the United Nation's Minamata Convention on Mercury has entered into force in August 2017 (UNEP, 2019). The Minamata

* Corresponding author.
E-mail: dywang@swu.edu.cn (D. Wang).

https://doi.org/10.1016/j.jes.2022.10.027
1001-0742/

Convention identified the need for research, development and monitoring (Article 19 and 20) of past and recent Hg levels in the environment.

The current main understanding of historical trends of Hg concentration and deposition is mainly derived from the various natural environmental archives, such as ice cores (Beal et al., 2015; Eyrikh et al., 2017; Kang et al., 2016; Kang et al., 2019b; Schuster, 2002), lake sediments (Drevnick et al., 2016; Engstrom et al., 2014; Sun et al., 2021; Yang, 2010), and peat bogs (Bao et al., 2016; Enrico et al., 2017; Zuna et al., 2012). However, these archives have their own limitations caused by their spatial distributions, differing altitude and climate, contrasting geochemical environments and the mixed information of Hg records (Bandara et al., 2019; Corella et al., 2017; Engstrom et al., 2014; Enrico et al., 2017; Navratil et al., 2018; Zdanowicz et al., 2016). Tree rings have been suggested as an emerging natural archive to reconstruct the historical atmospheric Hg trends due to their advantages of precise dating, high resolution, and wide geographical distribution (Binda et al., 2020; Clackett et al., 2018; Zhang et al., 2014). Tree-ring records of conifers have been successfully used to reconstruct historical changes in atmospheric Hg driven by local and regional emissions (Clackett et al., 2018, 2020; Ghotra et al., 2020; Kang et al., 2019a, 2018; Navratil et al., 2018; Peckham et al., 2019; Schneider et al., 2019; Wright et al., 2014).

The lack of long-term of measured atmospheric Hg concentration data leads impossible to directly validate the tree-ring reconstructed Hg trends (Arnold et al., 2018; Clackett et al., 2018; Navratil et al., 2018). Previous studies had different assessments on the suitability of using tree rings as the useful bioindicator for atmospheric Hg pollution. This is because the reliability of tree rings as records of environmental chemistry is species-, climate- and site-dependent (Arnold et al., 2018; Gustin et al., 2022; Novakova et al., 2021; Schneider et al., 2019; Wright et al., 2014).

The radial translocation and age effect (e.g., young trees have different Hg concentration trends in wood tissues) of tree rings are in debate currently in Hg dendrochemistry. Navratil et al. (2018) suggested little or no translocation of Hg within the European larch (*Larix decidua*) bole, but distinct radial translocation existed for some other tree species, like Scottish pine (*Pinus sylvestris*) (Novakova et al., 2021) and Whitebark pine (*Pinus albicaulis*) (Chellman et al., 2020). Results of Schneider et al. (2019) and Peckham et al. (2019) reported that the uptake atmospheric Hg efficiency by tree foliage largely differed among tree species and trees ages. Gustin et al. (2022) suggested that trees of the same age should be used when comparing tree-ring Hg concentrations across sites, and more work is needed to better understand the potential of Hg radial translocation in various tree species.

To date, many researchers are trying to explain the mechanism of radial translocation. Radial translocation of Hg is considered to occur throughout the sapwood rings (Cutter and Guyette, 1993; Siwik et al., 2010). This is because the active, live ray cells in the sapwood rings which allow water and nutrients to move radially could possibly transport Hg inwards (Arnold et al., 2018). Earlier studies postulated that radial translocation of trace metals in the xylem mainly contains two mechanisms: bi-directional diffusion and advection inwards (Okada et al., 2011; Watmough, 2002). Based on this hypothesis, Chellman et al. (2020) constructed an advection-diffusion model to explain discrepancies of elevated Hg events between co-located ice-core and tree-ring Hg records. Although this method is not based on the mechanism to explain the migration and transmission of Hg in tree rings, it provides evidence to test the potential of the radial translocation occurring.

Masson pine (*Pinus massoniana*) is a common and widespread tree species in forests of Southern China and Southeast Asia. The objective of this study was to evaluate the Hg source, radial translocation, and age effect, which are the fundamental to understand the suitability of Masson pine tree ring as a natural archive of atmospheric Hg. We examined the correlation between Masson pine tree-ring Hg and atmospheric Hg emission trends in Chongqing, and determined the divergence of atmospheric Hg uptake efficiency within inter and intra tree rings, and assessed the influence of tree age effect on reconstructing historical atmospheric Hg levels. Finally, an advection-diffusion model was used to quantify how the advection or diffusion within tree rings alters the atmospheric Hg signal preserved in tree rings.

1. Materials and methods

1.1. Sites description and sample collections

Our studied site locates at Mt. Jinyun, Chongqing Province, Southwestern China (29.84 °N, 106.40 °E). Chongqing is the largest industrial and commercial city in Southwest China, with a continuous growth of population and industries during last several decades. Mt. Jinyun is a national nature reserve, and 35 km away from the downtown of Chongqing. The weather is controlled by the subtropical monsoon humid climate, with an average annual temperature of 13.6°C and annual precipitation of 1,600 mm. The detailed information of the sampling site was shown in Appendix A Fig. S1.

In December of 2020, we sampled tree rings from 25 living Masson pine trees in a mixed broadleaf-conifer forest at Mt. Jinyun during the elevation of 480–530 m. Dual radii tree-ring cores of south-facing and west- or east- facing sides of each tree were collected at ~1 m height with a new 5.1-mm Haglöf increment borer and handled with nitrile gloves. The borer passed through the pith or through the early juvenile growth rings. The core samples were then sealed in the clean Teflon™ tubes with a diameter of 6-mm. We also sampled the tree disk samples to evaluate the Hg concentration variation along with the height of stem. We harvested 4 wind-fallen trees (WF-Tree) which still alive, and used the chainsaw to cut 3–5 disks (~3 cm thickness) at intervals of 2 or 5 meters along with the stem. The tree-disk samples were then placed in Ziploc bags to prevent the contamination.

1.2. Cross-dating and Hg analysis

In the laboratory, the tree-ring cores were dried in 50°C, oven for 2~3 days to remove adsorbed and interstitial water. An earlier study has shown that the oven drying at 50°C does not

lead to the Hg loss from woody biomass (Yang et al., 2017). After drying, 180- to 1500-grit sandpapers (Matador, Germany) were utilized to polish one side of the tree ring until the ring boundaries and cells clearly visible. The tree-ring widths were measured by a LINTAB^{TM}6 (Germany) with a precision of 0.001 mm. The quality of the cross-dating was checked using the COFECHA program to examine the absent or false rings in sampled tree ring cores. Then 28 tree cores (include 21 trees) without the absent or false rings were selected for subsequent analyses based on the coherence of the growth signal. The detailed information of the detrending chronology was shown in Appendix A Table S1.

Subsequently, 12 tree-ring cores from different trees across a range of calendar years from 1955 to 2020 were selected from 28 tree cores for Hg concentration analysis. Our protocol for choosing tree-ring cores for Hg analysis is that the core without any physical damage and the similarity in the time-length. The tree-ring cores were polished again to remove possible surface contamination from the cross-dating procedures before Hg measurements. Based on the tree-ring chronology, a stainless-steel blade was used to dissect the core into 5-year increments for Hg concentration measurements. The tree disks were soaked in ultrapure water for half an hour to remove possible impurities, and then dried in 50°C oven for 4-5 days. After drying, one side of the tree disks were polished by the same treatment of tree ring cores for dating, and then dissected into 1-year increments for Hg analysis. The detailed information of the sampled disks was in Appendix A Table S2.

We used the Milestone tri-cell Direct Mercury Analyzer (DMA-80, Italy) to determine the Hg concentration. Briefly, samples undergo thermal decomposition to release Hg from the matrix, and Hg is then preconcentrated using amalgamation, prior to detection by atomic absorption (Ghotra et al., 2020). Our calibration curve was generated by a 10-point dilution series of a certified aqueous Hg standard (High Purity Standards 1000 μg/mL Hg, 1 mol/L HNO_3), bracketing Hg amounts in both tree-ring samples and standard reference materials. Empty nickel boats and the certified reference material (CRM, GSB-27 of green onion) were determined three times respectively before daily sample measurements to evaluate analytical performance of DMA-80. During the sample measurement period, the CRM was measured once in every ten samples to assess the precision and stability of the DMA-80. The detection limit (0.01 ng Hg, $n = 36$ blanks) corresponded to a concentration of ~0.05–0.10 ng/g since all samples were weighted to ~0.1–0.2 g dry wood. The up to 166 measurements of CRM yielded a Hg concentration of 11.3±1.3 ng/g, which agreed with the certified value of 12.0±2.3 ng/g.

1.3. *Diffusion and advection modeling*

We used the advection-diffusion model (Chellman et al., 2020) to explore how Hg concentration shifted by advection or/and diffusion in tree rings. This model mainly contains the one-dimensional advection-diffusion equation:

$$\Delta C = D\frac{\partial C}{\partial x} + \mu\frac{\partial C}{\partial L} \quad (1)$$

where C (ng/g) is the tree-ring Hg concentration; x (mm) is the average width of tree rings in each year; L (mm) is the accumulated tree-ring distance from the current simulated year to the tree-ring in the heartwood; D (mm/year) is diffusion coefficient; μ (mm/year) is advection coefficient; ΔC (ng/g) is the annual change in Hg concentration after one step of advection-diffusion simulation. The model was run from 1961 to 2020 in 1-year time step with a fixed concentration at the inner boundary (1960).

If the Hg in tree rings mainly derived from atmosphere and without the radial translocation, the Hg concentration profile would be highly correlated to the trend of anthropogenic Hg emissions. Earlier studies have well documented that the cement production, steel and aluminum production, electricity and oil consumption, natural gas and coal consumption were the main sources for anthropogenic Hg emissions in Chongqing (Huang et al., 2017; Wu et al., 2016). Though the unknown of the detailed quantity of anthropogenic Hg emissions since 1960 in Chongqing, the temporal trends of these industrial activities can reflect the trend of anthropogenic emissions. Therefore, we calculated the integrated score (Appendix A Fig. S2, grey line) of these industrial activities mentioned above by principal component analysis (PCA) based on their annual productions, and selected the temporal score of first principal component. Subsequently, the score is converted to a positive value by the softmax conversion as the proxy index to represent temporal trend of anthropogenic Hg emissions in Chongqing. The initial condition of Hg concentration of advection-diffusion model was assumed to follow the similar decreasing gradient of the proposed proxy index for anthropogenic Hg emissions (Appendix A Fig. S2, black line).

Although we only had the proxy index of annual anthropogenic Hg emissions data between 1980 and 2020 in Chongqing, we assumed the annual anthropogenic Hg emissions during 1961−1980 should be comparable to the emissions of 1980. This is because the anthropogenic Hg emissions of China remained at a very low level before the reform and opening-up in 1978, specifically during years of the Great Cultural Revolution of 1966-1976 (Huang et al., 2017; Wu et al., 2016).

In Eq. (1), we proposed the bi-directional diffusion and the advection inwards along with ray parenchyma cells based on results from previous studies that postulated trace metal translocation from sapwood to heartwood (Okada et al., 2011; Watmough, 2002). We set three simulation scenarios: (1) diffusion alone occurs; (2) diffusion and advection occur simultaneously; (3) diffusion and advection occur simultaneously, but the advection coefficient varied with the tree ring age. We considered an age effect for the advection, but not for the diffusion. This is because the advection is driven by physiological processes, while the diffusion is driven by the concentration gradient (Cutter and Guyette, 1993; Hagemeyer, 1995).

We divided the whole simulation process into four periods (1961–1980, 1981–2000, 2001–2010, 2011–2020) which is based on the forestry industry standard of LY/T 2908−2017 for age-group division of natural Masson pine forest to reflect the age effect in scenario (3). Considering limited knowledge of how Hg is incorporated and preserved in the tree rings, values of D and μ in our model were randomly chosen in given ranges, and are not directly related to a physical mechanism. The diffusion coefficient D mainly ranged from 0 to 1.7 mm/year, and the range of μ from 0 to 3.0 mm/year through the iterative simu-

lation. This is because the negative Hg concentration occurred under the other selected ranges.

During the simulation, we used the exhaustive method to test the radial translocation among tree rings. More in detail, we evaluated the correlation (r value, Pearson correlation coefficient) between simulated temporal Hg concentration profile and the measured profile. Our criterial is that if more than 50% of measured profile can be explained by the model simulated radial translocation (i.e., $r^2 > 0.5$), we suggest a distinct radial translocation occurring among these tree rings. The final D and μ were obtained from the simulation which with the highest r.

1.4. *Uncertainties of the model*

It is noted that this advection-diffusion model is associated with distinct uncertainties. One is that D and μ in this model are not directly measured, and their values are determined by statistical methodology. In addition, the age-group division should depend on tree species and site location, the stage division in the model is only as the reference and may not be applicable to other tree species. Finally, due to the absence of the temporal trend of anthropogenic Hg emission inventories in Chongqing, we just used the temporal trends of main Hg emission industrial activities as the proxy to predict the initial Hg concentration profile in the model. Given the Hg dendrochemistry emerged recently and without any direct tools, this model still provides a new insight in understanding the Hg radial translocation and age effect of tree rings.

1.5. *Meteorological data*

Meteorological data were downloaded from the resource and environment science and data center (https://www.resdc.cn/). Meteorological variables included air pressure (daily mean), precipitation, relative humidity (daily mean), temperature (daily mean), wind speed (daily mean) and sunshine hours (SSH) during 1961 through 2020 of our studied site. Average 5-year data for each variable corresponding with the 5-year tree core segments were used for all subsequent analyses.

1.6. *Statistical methods*

Data were analyzed by using the statistical program R 3.6.3 and SPSS 26.0 with $P < 0.05$ as the level of statistical significance. The spline function detrending method in detrendeR package was used to remove the interference signals inside a single tree core. The synthesis of chronology which is a traditional method of dendrochronology to obtain the tree-ring width index and the simulation of advection-diffusion model were also performed in R. The principal component analysis by SPSS was used to reconstruct the potential anthropogenic Hg emission trend in Chongqing. Pearson correlation analysis was performed to determine the correlation among tree-ring Hg profiles and the correlation between tree-ring Hg profile and meteorological data. Paired sample t-test and One-way ANOVA were used to analyze the statistical difference of Hg concentration profile among different tree-ring cores. To determine the tree-specific variability of tree-ring Hg profiles, we assessed the variation of coefficient of variation (CV) for average tree-ring Hg concentrations along with the increasing tree-ring cores. The combn function in utils R package was used to calculate CV.

2. Results

2.1. *Hg records in tree cores*

The overall mean (±standard deviation) Hg concentration of tree-ring cores for 12 Masson pine trees over the period of 1955–2020 was 4.5±1.4 ng/g, with a range of 2.4–7.9 ng/g (Fig. 1). We observed distinct tree-specific differences in average tree-ring Hg concentration among Masson pine trees

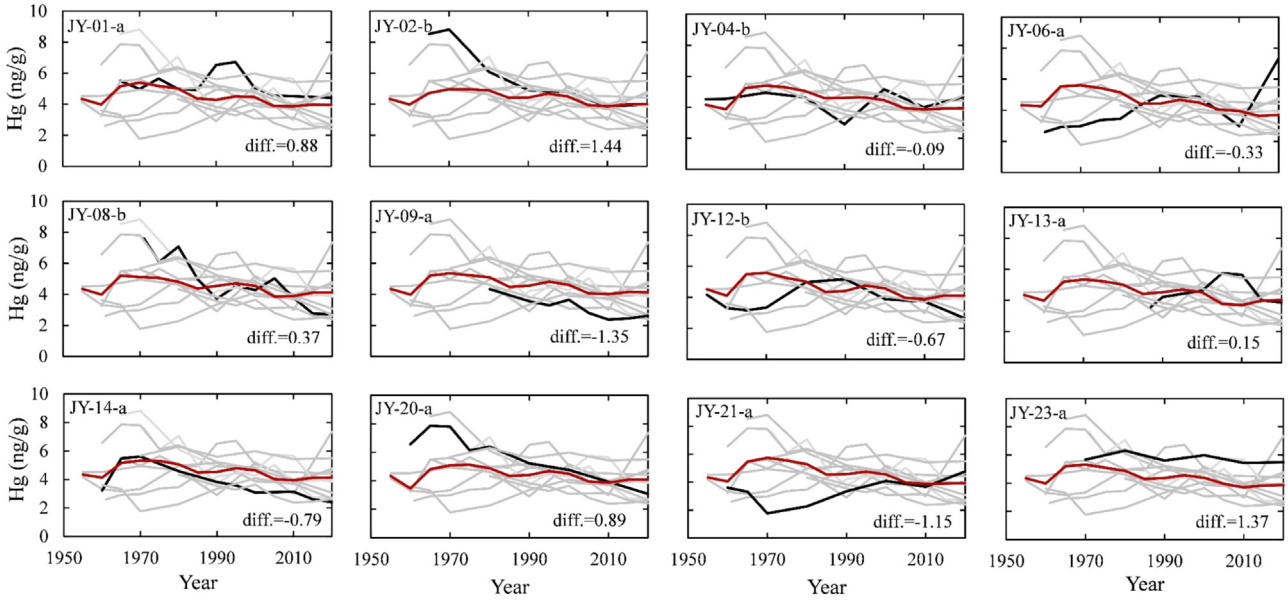

Fig. 1 – Comparisons of the individual raw tree-ring Hg records (black line; tree ID is indicated) against the other mean tree-ring records (red line) calculated from all other tree-ring Hg profiles (gray line). The "diff" refers to the difference for the mean Hg concentration between the individual record (red line) and the other mean record (black line).

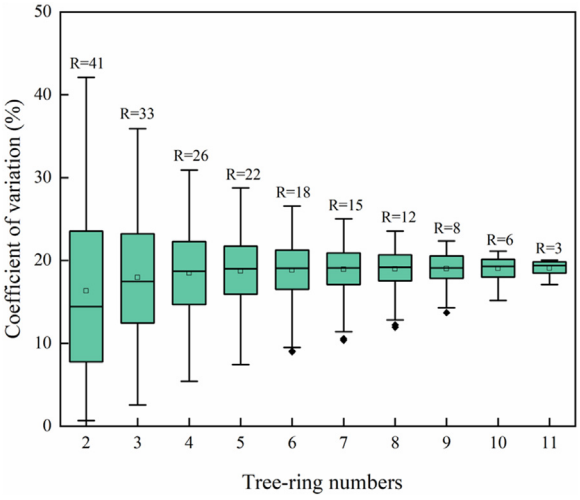

Fig. 2 – The variation of coefficient of variation (CV) of tree-ring Hg concentrations along with the tree-ring number. R represents the range (maximum - minimum) of CV.

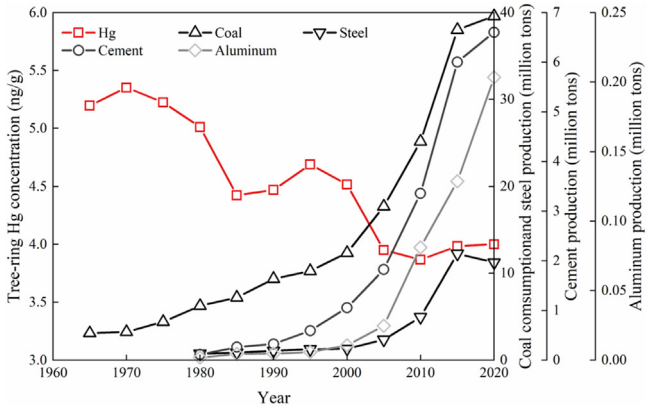

Fig. 3 – The temporal profiles of the average tree-ring Hg concentration against temporal trend of coal consumption, steel and aluminum production, and cement production of Chongqing since 1965.

(Fig. 1). For example, the tree-ring Hg concentration of tree JY-20-a was on average 0.9 ng/g higher than the other mean record (i.e., average value except for the selected tree-ring), and the tree-ring Hg concentration of tree JY-06-a was on average 0.3 ng/g lower than the record of other average. Mean differences between individual Hg series and the other average are large in absolute terms (ranging from 0.09 to 1.44 ng/g). Fig. 2 shows the decreasing of CV with the increasing tree-ring numbers. The R value (maximum - minimum) of the CV decreased to < 10% for the tree-ring cores >10.

The trend of average Hg concentration of 12 tree cores is shown in Fig. 3. The average tree-ring Hg concentration increased gradually from 1965, reaching a peak of 5.4 ng/g in 1970. During 1975–1985, the average tree-ring Hg concentration decreased gradually to 4.4 ng/g. Subsequently, the concentration began to rise slowly from 1990 and reached a small plateau of 4.7 ng/g in 1995, and then declined to a remained stable value of 4.0 ng/g after 2005. Coal combustion, cement production, steel and aluminum smelting are as the main sources of anthropogenic Hg emissions in Chongqing, and all of them increased exponentially since 1980.

Fig. 4 shows correlations between tree-ring Hg concentration and meteorological data. The tree-ring Hg concentration displayed the significantly negative correlation to the 5-year annual mean temperature ($r = -0.61$, $P < 0.05$, Fig. 2a), and the positive correlation to the 5-year annual mean SSH ($r = 0.82$, $P < 0.01$, Fig. 2b), while no significant correlation for other meteorological variables.

2.2. *Concentration at different trunk heights*

The overall mean Hg concentration of 19 Masson pine tree disks was 4.1±1.6 ng/g. Tree-ring concentrations in individual disks ranged from 1.8 to 9.2 ng/g, and the average Hg concentration of WF-Tree (Wind-fallen tree) 1, 2, 3 and 4 was 5.7, 3.2, 4.2 and 3.6 ng/g, with the significant difference respectively ($P < 0.05$, by One-Way ANOVA test, Fig. 5). The Hg temporal trends were consistent among tree heights (Fig. 5), and reached the peak of 5.0–9.0 ng/g during 1970–1990, then gradually decreased to 1.0–3.0 ng/g during 1990–2015 and continuously increased to 4.0–7.0 ng/g between 2015 and 2020.

Results of correlation of Hg concentration among different disks are displayed in Table 1. For WF-Tree 1 and WF-Tree 2, the disk along with the stem with 2-meter intervals, and with 5-meter interval for WF-Tree 3 and WF-Tree 4. We found that the Hg concentration of disk from the WF-Tree 1 (or 2) than WF-Tree 3 (or 4) showed a better correlation among each other, since most of correlation coefficients (r values) > 0.5.

The Hg concentrations of different disks from the same wind fallen tree in common growth period (1988–2020, 1981–2020, 1995–2020 and 2002–2020 for WF-Tree 1, 2, 3 and 4, respectively) are shown in Fig. 6. The average Hg concentration of WF-Tree 1, 2, 3 and 4 during the common growth period (1988–2020) was 5.5, 2.9, 4.0 and 3.8 ng/g, respectively, and these average values are significantly different among each other ($P < 0.05$, by One-Way ANOVA test, Appendix A Fig. S3). The disk Hg concentration gradually increased along with the stem height. There was no significant difference in the average Hg concentration between near two disks ($P < 0.05$, by paired sample t-test), such as between 4-1 and 4-2, between 4-4 and 4-5. However, the mean Hg concentration in the top disk was significantly 1–1.5 times of that in the bottom disk ($P < 0.05$, by paired sample t-test), such as between 2-1 and 2-5, between 4-1 and 4-5.

2.3. *Variations of Hg concentration for different tree age and modeling*

We combined the Hg concentration of increment cores and wind fallen tree disks to display the age effect. During the common growth period of 1990–2020 (Fig. 7), young trees aged 31–40 years had the highest Hg concentrations (average of 4.7 ng/g, with a range from 3.0 to 7.5 ng/g), followed by trees aged 41–60 years (average of 4.3 ng/g, with a range from 2.4 to 6.7 ng/g), and lowest Hg concentrations for trees aged 61–70 years

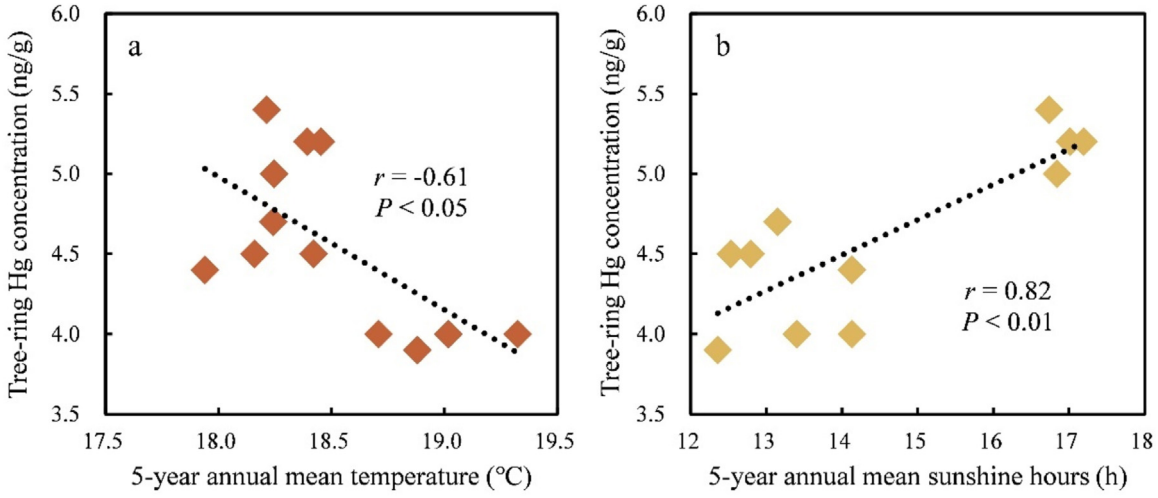

Fig. 4 – Correlations between tree-ring Hg concentration and 5-year annual mean temperature and 5-year annual mean sunshine hours from 1961 to 2020. *r* is the Pearson correlation coefficient.

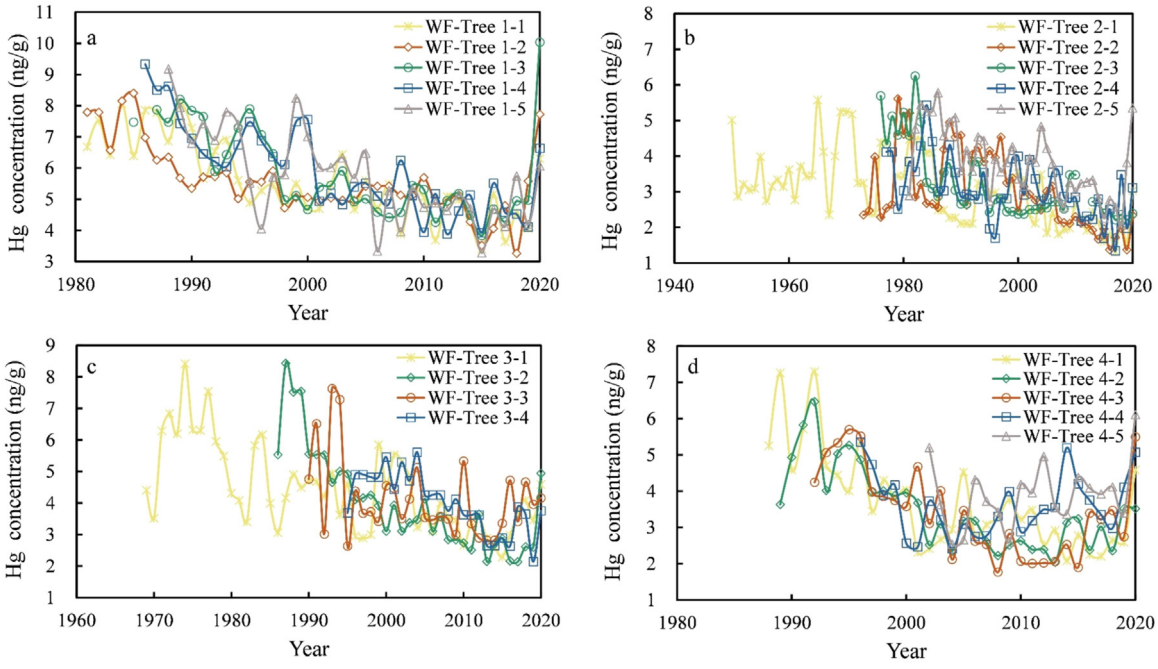

Fig. 5 – The variation trend of Hg concentration of tree disks. Disks 1–5 are numbered from the bottom of stem to the top stem.

(average of 3.8 ng/g, with a range from 2.3 to 5.2 ng/g). The difference of Hg concentrations between young trees aged 31–40 years and mature trees aged 61–70 years reached the significant level at the 95% confidence ($P < 0.05$, by One-Way ANOVA test).

The advection-diffusion model illustrated that only scenario (3) which with the tree age effect was in agreement with the measured Hg profile (Fig. 8). The correlation coefficient (*r*) between the simulated tree-ring Hg concentration and the measured tree-ring Hg concentration was up to 0.94 ($P < 0.001$, Fig. 8). The modeling results depicted that the diffusion coefficient *D* was 1.0 mm/year (1961–2020), and the advection coefficient μ ranged among 1.0–2.5 mm/year during 1961–2010, and 0.1 mm/year during 2011–2020.

3. Discussion

3.1. *Hg sources in tree rings*

Given most of heavy metals in tree rings derived from the root uptake and translocation via the xylem from root to stem (Watmough, 1999, 2002; Zayed et al., 1992), the concentration profile of heavy metals in tree rings cannot directly reflect the

Table 1 – Correlations of Hg concentrations among different disks from the same tree.

Disk number	WF-Tree 1-1	WF-Tree 1-2	WF-Tree 1-3	WF-Tree 1-4	WF-Tree 1-5	Disk number	WF-Tree 2-1	WF-Tree 2-2	WF-Tree 2-3	WF-Tree 2-4	WF-Tree 2-5
WF-Tree 1-1	1.000					WF-Tree 2-1	1.000				
WF-Tree 1-2	0.685**	1.000				WF-Tree 2-2	0.302*	1.000			
WF-Tree 1-3	0.736**	0.690**	1.000			WF-Tree 2-3	0.649**	0.324*	1.000		
WF-Tree 1-4	0.660**	0.574**	0.658**	1.000		WF-Tree 2-4	0.574**	0.175	0.355*	1.000	
WF-Tree 1-5	0.740**	0.362*	0.529**	0.684**	1.000	WF-Tree 2-5	0.484**	0.308	0.346*	0.507**	1.000
Disk number	WF-Tree 3-1	WF-Tree 3-2	WF-Tree 3-3	WF-Tree 3-4		Disk number	WF-Tree 4-1	WF-Tree 4-2	WF-Tree 4-3	WF-Tree 4-4	WF-Tree 4-5
WF-Tree 3-1	1.000					WF-Tree 4-1	1.000				
WF-Tree 3-2	0.396*	1.000				WF-Tree 4-2	0.701**	1.000			
WF-Tree 3-3	0.200	0.360*	1.000			WF-Tree 4-3	0.536**	0.739**	1.000		
WF-Tree 3-4	0.429*	0.467*	0.282	1.000		WF-Tree 4-4	0.309	0.447*	0.380	1.000	
						WF-Tree 4-5	-0.022	0.190	0.392	0.332	1.000

* Correlation is significant at $P < 0.05$ level;
** Correlation is significant at $P < 0.01$ level.

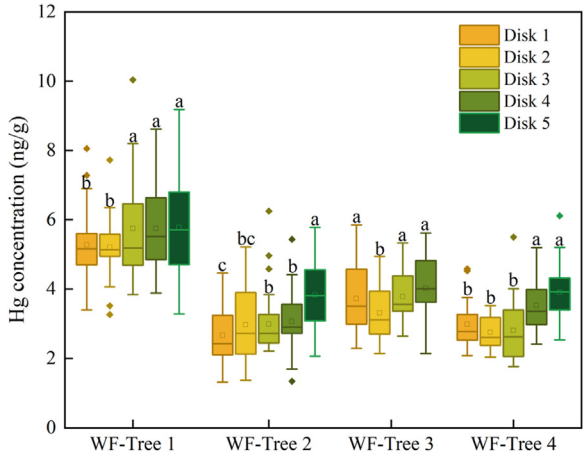

Fig. 6 – Hg concentrations of different disks among each sampled wind-fallen tree. Disks 1–5 are numbered from the bottom of stem to the top stem, and Hg concentrations are compared in common growth period of each group respectively. Different letters represent statistical differences within groups at the 95% confidence level ($P < 0.05$).

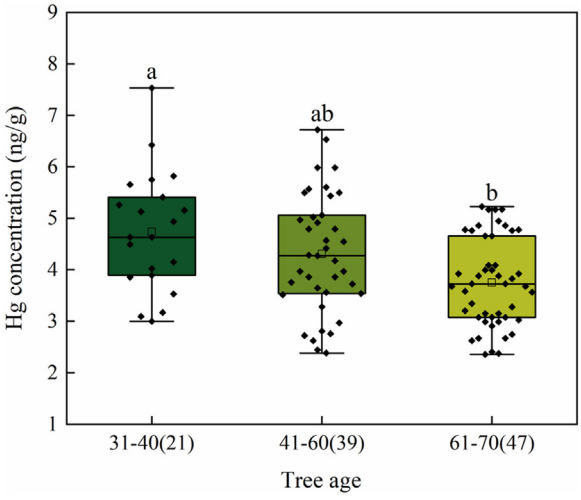

Fig. 7 – Hg concentrations of different age trees during the common growth period (1990–2020). Different letters represent statistical differences among groups at the 95% confidence level ($P < 0.05$), and the numbers in brackets represent the number of samples.

temporal variation of atmospheric concentrations or deposition fluxes. This is because the depth and chemistry of the soil and the root structure would influence amounts and sources (e.g., rock weathering processes and atmospheric depositions) of heavy metal stored in woods. These factors result in the mismatch of the environmental changes and records in tree rings (Watmough, 2002; Zayed et al., 1992).

Unlike most of heavy metals as the particle bounded form in the atmosphere, more than 95% of Hg in the atmosphere is in the form of gaseous elemental mercury (Hg^0) (Sprovieri et al., 2016; Zhang et al., 2019). Atmospheric Hg^0 can enter leaves via both stomatal and nonstomatal pathways, and subsequently translocated to tree rings through phloem and xylem (Arnold et al., 2018; Laacouri et al., 2013; Naharro et al., 2020; Stamenkovic, 2009). Additionally, field and experimental measurements indicated that up to 90% Hg in the root zone is bound to the cell walls and membranes of fine roots during the uptake process (Cui et al., 2014; Wang et al., 2012), and only a small amount of Hg in roots (<5%) can be translocated into the aboveground woody biomass (Arnold et al., 2018; Graydon et al., 2006; Greger et al., 2005; Wang et al., 2021). Moreover, the controlled dose-response experimental results (Arnold et al., 2018) showed that tree-ring Hg concentrations of *Pinus* trees were primarily influenced by air Hg concentrations but not soil Hg concentrations. The Hg isotopic evidence also further confirmed atmospheric Hg^0 as the dominant source in woody biomass (Wang et al., 2020).

Consistent with previous results, our data also reveal that Hg in tree rings mainly from atmospheric Hg sources by canopy foliage uptake. Fig. 6 shows that tree-disk Hg con-

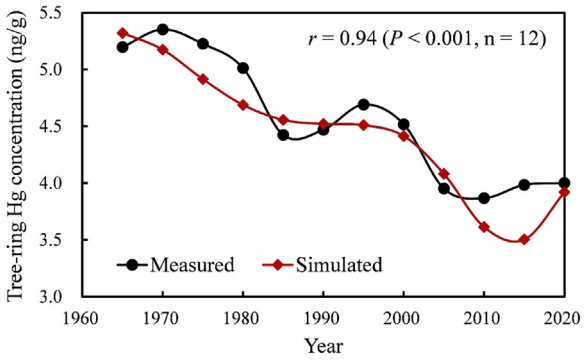

Fig. 8 – The correlation between measured temporal tree-ring Hg concentration profile (black) and simulated Hg concentration profile (red). *r* is the Pearson correlation coefficient. Such simulation is driven with the diffusion coefficient D = 1.0 mm/year (1961–2020), and advection coefficient μ_1 = 2.5 mm/year (1961–1980), μ_2= 1.5 mm/year (1981–2000), μ_3= 1.0 mm/year (2001–2010) and μ_4= 0.1 mm/year (2011–2020).

centration significantly increased along with the height of stem, indicating that the Hg transport from canopy to woody biomass after foliage uptake of atmospheric Hg. However, whether the Masson pine tree rings can regard as a useful archive, we need to further evaluate impacts from other factors which influencing uptake Hg transport and allocation in trees.

3.2. *Influence of environmental factors on tree-ring Hg concentration*

We observed the distinct tree-specific variations both in Masson pine tree-ring Hg profiles (Fig. 1) and disk Hg records (Fig. 5, Table 1). Previous studies suggested to reduce tree-specific variabilities by increasing the tree-ring samples in Hg dendrochemistry (Peckham et al., 2019; Schneider et al., 2019). We can obtain a valid and consistent Hg concentration trend when ≥10 tree-ring cores since <10% difference of their CV (R value in Fig. 2).

Causes of tree-specific differences are not well known, but may be associated with impacts from the local environmental conditions. The local meteorological factors could result in the variation of air Hg exposures, such as relative humidity (Choi and Holsen, 2009) and wind speed (Fu, 2010), which have been shown to be inversely correlated to atmospheric Hg concentrations in certain environments. Trees located below the prevailing wind direction of pollution sources may accumulate more Hg due to the higher atmospheric concentration (Schneider et al., 2019). Environmental and meteorological factors also have impact on the tree physiology, especially the impact on stomatal density and conductance, thus affecting the uptake of atmospheric Hg by leaves. For example, several studies reported that the local variation of atmospheric relative humidity could result in a change of stomatal conductance, thus subsequently influencing Hg assimilation into tree tissues (Arnold et al., 2018; Gustin et al., 2022; Stamenkovic, 2009). Gustin et al. (2022) also found that meteorological factors, including dew point, temperature and relative humidity were negatively correlated with ring Hg concentrations.

In our study, we also reveal the fact that the local environmental conditions influencing the tree-ring Hg variations, since the tree-ring Hg concentration with the significantly negative correlation to temperature and positive correlation to SSH (i.e., sunshine hours, Fig. 4). This is because the higher temperature leads to the close of foliage stomata, while the increase of SSH promotes the time of stomata opening, thus influencing the Hg assimilation into tree tissues (Gustin et al., 2022).

3.3. *Influence of age effect on tree-ring Hg concentration*

Tree physiological factors, that affect the uptake of atmospheric Hg by leaves and Hg translocation via phloem and xylem, also influence the variation of tree-ring Hg concentration profiles. These physiological factors include, but are not limited to stomatal and epidermal properties and composition, leaf area, tree ages, tree height, and canopy dynamics (Arnold et al., 2018; Chellman et al., 2020; Clackett et al., 2018; Laacouri et al., 2013; Schneider et al., 2019). In this study, more attention is paid to the tree age among these physiological factors. This is because tree age is a straightforward parameter obtained from tree-ring counting, but as a useful indicator to present the comprehensive influence of other factors which related to the tree growth, e.g., canopy structure and height, stomatal conductance and epidermal properties, etc. (England and Attiwill, 2005; Niinemets, 2002; Peckham et al., 2019; Schneider et al., 2019; Stoffberg et al., 2008).

The Hg concentration in tree rings during common growth periods decreasing with the increasing tree age (Fig. 7) demonstrates a distinct tree age effect in Masson pine tree rings. Several reasons can explain this age effect. One is that young trees are more sensitive to the variation of atmospheric Hg concentration. The young trees have higher stomatal conductance and enzyme activity (Hubbard, 1999), therefore greater atmospheric Hg assimilation (Peckham et al., 2019) and radial translocation rates in vegetation (more in detail in the following section). In addition, cuticular uptake often decreases with tissue age since cuticular properties such as the sorption sites in cuticles is controlled by the tissue age (Schneider et al., 2019; Schreiber, 2005). Another reason is that the tree age could reflect the dilution effect (Scanlon et al., 2020) of woody biomass. The fast rate of wood biomass increment during the young growth period leads to a more distinct dilution effect than the mature tree growth period (Gustin et al., 2022; Wang et al., 2021b). Such a dilution effect likely results in the Hg concentration more variable during the young growth period of trees. Finally, the young tree with the lower canopy height shortens the Hg transportation distance from canopy to the stem, thus leading to the elevated Hg concentration in the young tree rings (Wang et al., 2021a; Yanai et al., 2020). Ahn et al. (2020) suggested that higher tree-ring Hg concentration in the young period was influenced by soil Hg concentration by root. However, this explanation is likely not the cause for the age effect, since the recent study has provided strong evidences to show that root uptake of Hg hardly contributes to Hg sources in stem (Yuan et al., 2022). Several studies have in-

dicated that trees of similar age should be sampled when comparing tree-ring Hg concentrations across sites (Gustin et al., 2022; Peckham et al., 2019; Watmough, 1999). Herein, we suggest that the tree-ring Hg profile of the young growth period (generally 30–40 years) is doubtable to reflect the trend of atmospheric Hg concentration in Hg dendrochemistry.

3.4. *Radial translocation*

Our results showed that the opposite trend of Hg concentration in Masson pine tree rings compared to trends of anthropogenic indexes in Chongqing (Fig. 3). Besides the influencing factors discussed above, we also propose that the radial translocation contribute to such variabilities of Hg concentrations in tree rings. The advection-diffusion model illustrates that only scenario (3) that the advection-diffusion model with tree age effect is in agreement with the measured Hg profile (Fig. 8). Interestingly, more than 10-time higher advection coefficient μ during the young growth period (1961−2010) than the mature growth period (>2010) is consistent with the Hg isotopic data of Masson pine tree rings (about 130 years), which exhibited that the radial translocation mainly occurred in the fast-growing period, not mainly in the mature growth period (Wang et al., 2021b). Hence, our results again support that the Hg concentration profile of the earlier 30- to 40-year tree rings cannot reflect the historical atmospheric Hg trends due to the strongly radial translocation occurring. The distinct radial translocation existed in tree rings during the young growth period can be attributed to the higher nutrient and water translocations by ray-cell incidentally promoting the Hg translocation (Meerts, 2002; Novakova et al., 2021; Sands and Mulligan, 1990).

Our results also depict that the advection has the higher impact than diffusion in controlling the variation of Hg concentration among tree rings since the simulated Hg showed a small shift when increasing the D from 0.5 to 1.5 (Appendix A Fig. S4a), but with a distinct variation when increasing the μ from 0.1 to 2.5 (Appendix A Fig. S4b). Such a similar result is also displayed in the earlier study (Chellman et al., 2020). Differently, Chellman et al. (2020) suggested a 1.0 mm/year advection coefficient for Whitebark pine tree rings, which much lower than the values of this study (1.5–2.5 mm/year) during the young growth period of trees. This indicates that the advection coefficient varies greatly among tree species, and is highly related to the tree ring physiological structure.

4. Conclusions

Our results demonstrate that foliar uptake of atmospheric Hg is the main source of Hg in tree rings, however, environmental and physiological factors lead to the distinct tree-specific Hg concentration in Masson pine tree rings. The advection-diffusion model further elucidates that the advection induced Hg radial translocation during the young growth period of trees mainly plays an important role in shaping the Hg variabilities of tree rings. Therefore, our results suggest that the Hg concentration profile of Masson pine tree ring is not a promising index to reflect the historical atmospheric Hg concentration trend. However, we do not negate the potential of using tree ring to reflect the historical atmospheric Hg variation. In fact, our study points out the challenge of Hg dendrochemistry, that how to address the noise signal caused by the environmental and tree physiological impacts on Hg uptake and translocation in vegetation. Hence, we recommend further studies to focus on issues of understanding Hg translocation processes, specifically the mechanism of radial translocation in the tree rings. This would largely improve the reliable of Hg dendrochemistry.

Our results also have two methodological recommendations for Hg dendrochemistry: (1) Increasing the tree-ring cores (tree numbers ≥ 10) can remarkedly reduce the tree-specific variabilities of Hg concentration profiles which is caused by the tree physiological and environmental factors. (2) The tree-ring Hg concentration profile of the young growth period (generally 30–40 years) of Masson pine tree is likely untrusted to reflect the temporal variation of atmospheric Hg due to the potential radial translocation and the age effect.

Declaration of Competing Interest

The authors declare that they have no known competing financial interests or personal relationships that could have appeared to influence the work reported in this article.

Acknowledgments

This work was supported by the Natural Science Foundation of Chongqing (No. cstc2020jcyj-msxmX0063) and the National Natural Science Foundation of China (No. 41977272). Thanks for Mr. Boning Bing and Miss Yiwei Wang for their great help in sampling collection and measurements.

Appendix A Supplementary data

Supplementary material associated with this article can be found, in the online version, at doi:10.1016/j.jes.2022.10.027.

REFERENCES

Ahn, Y.S., Jung, R., Moon, J.H., 2020. Approaches to understand historical changes of mercury in tree rings of Japanese Cypress in Industrial Areas. Forests 11, 800.

Arnold, J., Gustin, M.S., Weisberg, P.J., 2018. Evidence for nonstomatal uptake of Hg by Aspen and translocation of Hg from foliage to tree rings in Austrian pine. Environ. Sci. Technol. 52, 1174–1182.

Bandara, S., Froese, D.G., St. Louis, V.L., Cooke, C.A., Calmels, F., 2019. Postdepositional mercury mobility in a permafrost peatland from central Yukon, Canada. ACS Earth Sp. Chem. 3, 770–778.

Bao, K., Shen, J., Wang, G., Sapkota, A., McLaughlin, N., 2016. Estimates of recent Hg pollution in northeast China using peat profiles from Great Hinggan Mountains. Environ. Earth Sci. 75, 536.

Beal, S.A., Osterberg, E.C., Zdanowicz, C.M., Fisher, D.A., 2015. Ice core perspective on mercury pollution during the past 600 years. Environ. Sci. Technol. 49, 7641–7647.

Binda, G., Di Iorio, A., Monticelli, D., 2020. The what, how, why, and when of dendrochemistry: (paleo) environmental information from the chemical analysis of tree rings. Sci. Total Environ. 758, 143672.
Chellman, N., Csank, A., Gustin, M.S., Arienzo, M.M., Vargas Estrada, M., McConnell, J.R., 2020. Comparison of co-located ice-core and tree-ring mercury records indicates potential radial translocation of mercury in whitebark pine. Sci. Total Environ. 743, 140695.
Chen, C.Y., Driscoll, C.T., Eagles-Smith, C.A., Eckley, C.S., Gay, D.A., Hsu-Kim, H., et al., 2018. A critical time for mercury science to inform global policy. Environ. Sci. Technol. 52, 9556–9561.
Choi, H.D., Holsen, T.M., 2009. Gaseous mercury fluxes from the forest floor of the Adirondacks. Environ. Pollut. 157, 592–600.
Clackett, S.P., Porter, T.J., Lehnherr, I., 2018. 400-year record of atmospheric mercury from tree-rings in northwestern Canada. Environ. Sci. Technol. 52, 9625–9633.
Clackett, S.P., Porter, T.J., Lehnherr, I., 2020. The tree-ring mercury record of Klondike gold mining at Bear Creek, central Yukon. Environ. Pollut. 268, 115777.
Corella, J.P., Valero-Garcés, B.L., Wang, F., Martínez-Cortizas, A., Cuevas, C.A., Saiz-Lopez, A., 2017. 700 years reconstruction of mercury and lead atmospheric deposition in the Pyrenees (NE Spain). Atmos. Environ. 155, 97–107.
Cui, L.W., Feng, X.B., Lin, C.J., Wang, X.M., Meng, B., Wang, X., et al., 2014. Accumulation and translocation of 198Hg in four crop species. Environ. Toxicol. Chem. 33, 334–340.
Cutter, B.E., Guyette, R.P., 1993. Anatomical, chemical, and ecological factors affecting tree species choice in dendrochemistry studies. J. Environ. Qual. 22, 611–619.
Drevnick, P.E., Cooke, C.A., Barraza, D., Blais, J.M., Coale, K.H., Cumming, B.F., et al., 2016. Spatiotemporal patterns of mercury accumulation in lake sediments of western north America. Sci. Total Environ. 568, 1157–1170.
England, J.R., Attiwill, P.M., 2005. Changes in leaf morphology and anatomy with tree age and height in the broadleaved evergreen species, Eucalyptus regnans F. Muell. Trees 20, 79–90.
Engstrom, D.R., Fitzgerald, W.F., Cooke, C.A., Lamborg, C.H., Drevnick, P.E., Swain, E.B., et al., 2014. Atmospheric Hg emissions from preindustrial gold and silver extraction in the Americas: A reevaluation from lake-sediment archives. Environ. Sci. Technol. 48, 6533–6543.
Enrico, M., Le Roux, G., Heimburger, L.E., Van Beek, P., Souhaut, M., Chmeleff, J., et al., 2017. Holocene atmospheric mercury levels reconstructed from peat bog mercury stable isotopes. Environ. Sci. Technol. 51, 5899–5906.
Eyrikh, S., Eichler, A., Tobler, L., Malygina, N., Papina, T., Schwikowski, M., 2017. A 320 year ice-core record of atmospheric Hg pollution in the Altai, central Asia. Environ. Sci. Technol. 51, 11597–11606.
Fu, X.W.F., X, Dong, Z.Q., Yin, R.S., Wang, J.X., Yang, Z.R., Zhang, H., 2010. Atmospheric gaseous elemental mercury (GEM) concentrations and mercury depositions at a high-altitude mountain peak in south China. Atmos. Chem. Phys. 10, 2425–2437.
Ghotra, A., Lehnherr, I., Porter, T.J., Pisaric, M.F.J., 2020. Tree-ring inferred atmospheric mercury concentrations in the Mackenzie Delta (NWT, Canada) peaked in the 1970s but are increasing once more. ACS Earth Sp. Chem. 4, 457–466.
Graydon, J.A., St Louis, V.L., Lindberg, S.E., Hintelmann, H., Krabbenhoft, D.P., 2006. Investigation of mercury exchange between forest canopy vegetation and the atmosphere using an new dynamic chamber. Environ. Sci. Technol. 40, 4780–4788.
Greger, M., Wang, Y., Neuschutz, C., 2005. Absence of Hg transpiration by shoot after Hg uptake by roots of six terrestrial plant species. Environ. Pollut. 134, 201–208.
Gustin, M.S., Ingle, B., Dunham-Cheatham, S.M., 2022. Further investigations into the use of tree rings as archives of atmospheric mercury concentrations. Biogeochemistry 93.
Hagemeyer, J., Schafer, H., 1995. Seasonal variations in concentrations and radial distribution patterns of Cd, Pb and Zn in stem wood of beech trees (*Fagus sylvatica* L.). Sci. Total Environ. 166, 77–87.
Huang, Y., Deng, M., Li, T., Japenga, J., Chen, Q., Yang, X., et al., 2017. Anthropogenic mercury emissions from 1980 to 2012 in China. Environ. Pollut. 226, 230–239.
Hubbard, R.M., Bond, B.J., Ryan, M.G., 1999. Evidence that hydraulic conductance limits photosynthesis in old Pinus ponderosa trees. Tree Physiol 19, 165–172.
Kang, H.H., Liu, X.H., Guo, J.M., Wang, B., Xu, G.B., Wu, G.J., et al., 2019a. Characterization of mercury concentration from soils to needle and tree rings of Schrenk spruce (Picea schrenkiana) of the middle Tianshan Mountains, northwestern China. Ecol. Indic. 104, 24–31.
Kang, H.H., Liu, X.H., Guo, J.M., Xu, G.B., Wu, G.J., Zeng, X.M., et al., 2018. Increased mercury pollution revealed by tree rings from the China's Tianshan Mountains. Sci. Bull. 63, 1328–1331.
Kang, S.C., Huang, J., Wang, F.Y., Zhang, Q.G., Zhang, Y.L., Li, C.L., et al., 2016. Atmospheric mercury depositional chronology reconstructed from lake sediments and ice core in the Himalayas and Tibetan Plateau. Environ. Sci. Technol. 50, 2859–2869.
Kang, S.C., Zhang, Q.G., Qian, Y., Ji, Z.M., Li, C.L., Cong, Z.Y., et al., 2019b. Linking atmospheric pollution to cryospheric change in the Third Pole region: current progress and future prospects. Natl. Sci. Rev. 6, 796–809.
Laacouri, A., Nater, E.A., Kolka, R.K., 2013. Distribution and uptake dynamics of mercury in leaves of common deciduous tree species in Minnesota, U.S.A. Environ. Sci. Technol. 47, 10462–10470.
Lehnherr, I., 2014. Methylmercury biogeochemistry: a review with special reference to Arctic aquatic ecosystems. Environ. Rev. 22, 229–243.
Meerts, P., 2002. Mineral nutrient concentrations in sapwood and heartwood: a literature review. Ann. For. Sci. 59, 713–722.
Naharro, R., Esbri, J.M., Amoros, J.A., Higueras, P.L., 2020. Experimental assessment of the daily exchange of atmospheric mercury in Epipremnum aureum. Environ. Geochem. Health 42, 3185–3198.
Navratil, T., Novakova, T., Shanley, J.B., Rohovec, J., Matouskova, S., Vankova, M., et al., 2018. Larch tree rings as a tool for reconstructing 20th century central European atmospheric mercury trends. Environ. Sci. Technol. 52, 11060–11068.
Niinemets, Ü., 2002. Stomatal conductance alone does not explain the decline in foliar photosynthetic rates with increasing tree age and size in Picea abies and Pinus sylvestris. Tree Physiol 22, 515–535.
Novakova, T., Navratil, T., Demers, J.D., Roll, M., Rohovec, J., 2021. Contrasting tree ring Hg records in two conifer species: multi-site evidence of species-specific radial translocation effects in Scots pine versus European larch. Sci. Total Environ. 762, 144022.
Okada, N., Hirakawa, Y., Katayama, Y., 2011. Radial movement of sapwood-injected rubidium into heartwood of Japanese cedar (*Cryptomeria japonica*) in the growing period. J. Wood. Sci. 58, 1–8.
Peckham, M.A., Gustin, M.S., Weisberg, P.J., 2019. Assessment of the suitability of tree rings as archives of global and regional atmospheric mercury pollution. Environ. Sci. Technol. 53, 3663–3671.
Sands, R., Mulligan, D.R., 1990. Water and nutrient dynamics and tree growth. Forest. Ecol. Manag. 30, 91–111.
Scanlon, T.M., Riscassi, A.L., Demers, J.D., Camper, T.D., Lee, T.R., Druckenbrod, D.L., 2020. Mercury accumulation in tree rings: observed trends in quantity and isotopic composition in

Shenandoah National Park, Virginia. J. Geophys. Res. Biogeosciences 125.
Schneider, L., Allen, K., Walker, M., Morgan, C., Haberle, S., 2019. Using tree rings to track atmospheric mercury pollution in Australia: the legacy of mining in Tasmania. Environ. Sci. Technol. 53, 5697–5706.
Schreiber, L., 2005. Polar paths of diffusion across plant cuticles: new evidence for an old hypothesis. Ann. Bot. 95, 1069–1073.
Schuster, P.F.K.D.P., Naftz, D.L., Cecil, L.D., Olson, M.L., Dewild, J.F., Susong, D.D., et al., 2002. Atmospheric mercury deposition during the last 270 years: A glacial ice core record of natural and anthropogenic sources. Environ. Sci. Technol. 36, 2303–2310.
Shah, V., Jacob, D.J., Thackray, C.P., Wang, X., Sunderland, E.M., Dibble, T.S., et al., 2021. Improved mechanistic model of the atmospheric redox chemistry of mercury. Environ. Sci. Technol. 55, 14445–14456.
Siwik, E.I., Campbell, L.M., Mierle, G., 2010. Distribution and trends of mercury in deciduous tree cores. Environ. Pollut. 158, 2067–2073.
Sprovieri, F., Pirrone, N., Bencardino, M., D'Amore, F., Carbone, F., Cinnirella, S., et al., 2016. Atmospheric mercury concentrations observed at ground-based monitoring sites globally distributed in the framework of the GMOS network. Atmos. Chem. Phys. 16, 11915–11935.
Stamenkovic, J.G., M, S., 2009. Nonstomatal versus stomatal uptake of atmospheric mercury. Environ. Sci. Technol. 43, 1367–1372.
Stoffberg, G.H., van Rooyen, M.W., van der Linde, M.J., Groeneveld, H.T., 2008. Predicting the growth in tree height and crown size of three street tree species in the City of Tshwane, South Africa. Urban For. Urban Green. 7, 259–264.
Streets, D.G., Horowitz, H.M., Jacob, D.J., Lu, Z., Levin, L., Ter Schure, A.F.H., et al., 2017. Total mercury released to the environment by human activities. Environ. Sci. Technol. 51, 5969–5977.
Sun, R.Y., Sun, G.Y., Kwon, S.Y., Feng, X.B., Kang, S.C., Zhang, Q.G., et al., 2021. Mercury biogeochemistry over the Tibetan Plateau: an overview. Crit. Rev. Env. Sci. Tec 51, 577–602.
UNEP, 2019. Global mercury assessment 2018, in: Programme, U.N.E. (Ed.). Chemicals and health branch: Geneva, Switzerland.
Wang, J.J., Guo, Y.Y., Guo, D.L., Yin, S.L., Kong, D.L., Liu, Y.S., et al., 2012. Fine root mercury heterogeneity: metabolism of lower-order roots as an effective route for mercury removal. Environ. Sci. Technol. 46, 769–777.
Wang, X., Yuan, W., Lin, C.-J., Feng, X.B., 2021. Mercury cycling and isotopic fractionation in global forests. Crit. Rev. Env. Sci. Tec 1–24.
Wang, X., Yuan, W., Lin, C.-J., Luo, J., Wang, F.Y., Feng, X.B., et al., 2020. Underestimated sink of atmospheric mercury in a deglaciated forest chronosequence. Environ. Sci. Technol. 54, 8083–8093.
Wang, X., Yuan, W., Lin, C.-J., Wu, F., Feng, X.B., 2021. Stable mercury isotopes stored in Masson Pinus tree rings as atmospheric mercury archives. J. Hazard. Mater. 415.
Watmough, S.A., 1999. Monitoring historical changes in soil and atmospheric trace metal levels by dendrochemical analysis. Environ. Pollut. 106, 391–403.
Watmough, S.A., Hutchinson, T.C, 2002. Historical changes in lead concentrations in tree-rings of sycamore, oak and Scots pine in north-west England. Environ. Sci. Technol. 293, 85–96.
Wright, G., Woodward, C., Peri, L., Weisberg, P.J., Gustin, M.S., 2014. Application of tree rings [dendrochemistry] for detecting historical trends in air Hg concentrations across multiple scales. Biogeochemistry 120, 149–162.
Wu, Q.R., Wang, S.X., Li, G.L., Liang, S., Lin, C.-J., Wang, Y.F., et al., 2016. Temporal trend and spatial distribution of speciated atmospheric mercury emissions in China during 1978-2014. Environ. Sci. Technol. 50, 13428–13435.
Yanai, R.D., Yang, Y., Wild, A.D., Smith, K.T., Driscoll, C.T., 2020. New approaches to understand mercury in trees: radial and longitudinal patterns of mercury in tree rings and genetic control of mercury in maple sap. Water Air Soil Pollut 231, 1–10.
Yang, H.B.R.W., Turner, S.D., Rose, N.L., Derwent, R.G., Wu, G., Yang, R., 2010. Historical reconstruction of mercury pollution across the Tibetan Plateau using lake sediments. Environ. Sci. Technol. 44, 2918–2924.
Yang, Y., Yanai, R.D., Montesdeoca, M., Driscoll, C.T., 2017. Measuring mercury in wood: challenging but important. Int. J. Environ. Anal. Chem. 97, 456–467.
Yuan, W., Wang, X., Lin, C.-J., Wu, F., Luo, K., Zhang, H., et al., 2022. Mercury uptake, accumulation, and translocation in roots of subtropical forest: Implications of global mercury budget. Environ. Sci. Technol..
Zayed, J., Loranger, S., Kennedy, G., 1992. Variations of trace-element concentrations in red spruce tree rings. Water Air Soil Pollut 65, 281–291.
Zdanowicz, C.M., Krümmel, E.M., Poulain, A.J., Yumvihoze, E., Chen, J., Štrok, M., et al., 2016. Historical variations of mercury stable isotope ratios in Arctic glacier firn and ice cores. Glob. Biogeochem. Cycles 30, 1324–1347.
Zhang, L., Zhou, P.S., Cao, S.Z., Zhao, Y., 2019. Atmospheric mercury deposition over the land surfaces and the associated uncertainties in observations and simulations: a critical review. Atmos. Chem. Phys. 19, 15587–15608.
Zhang, T.W., Yuan, Y.J., He, Q., Wei, W.S., Diushen, M., Shang, H.M., et al., 2014. Development of tree-ring width chronologies and tree-growth response to climate in the mountains surrounding the Issyk-Kul Lake, central Asia. Dendrochronologia 32, 230–236.
Zuna, M., Ettler, V., Sebek, O., Mihaljevic, M., 2012. Mercury accumulation in peatbogs at Czech sites with contrasting pollution histories. Environ. Sci. Technol. 424, 322–330.